IEEE Photonics Journal
An IEEE Photonics Society Publication

Open Access

Pupil Size Estimation Based on Spatially Weighted Corneal Flux Density

Volume 11, Number 6, December 2019

Yuning Zhang
Shuai Li
Jiang Wang
Ping Wang
Yan Tu
Xiaohua Li
Baoping Wang

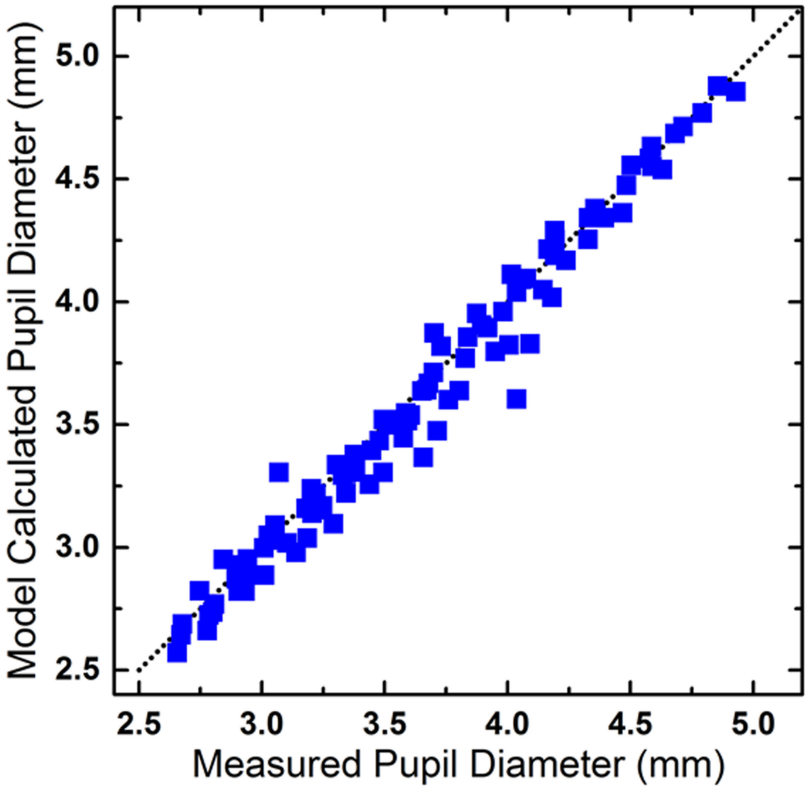

DOI: 10.1109/JPHOT.2019.2948223

IEEE photonics SOCIETY

IEEE

Pupil Size Estimation Based on Spatially Weighted Corneal Flux Density

Yuning Zhang, Shuai Li, Jiang Wang, Ping Wang, Yan Tu, Xiaohua Li, and Baoping Wang

Joint International Research Laboratory of Information Display and Visualization, School of Electronic Science & Engineering, Southeast University, Nanjing 210096, China

DOI:10.1109/JPHOT.2019.2948223

Manuscript received September 1, 2019; revised October 14, 2019; accepted October 16, 2019. Date of publication October 18, 2019; date of current version November 26, 2019. The work was supported in part by the National Key R&D Program of China under Grant 2016YFB0401201 and in part by the Nanjing Industry Academia Research Funding under Grant 201722003. Corresponding author: Yuning Zhang (e-mail: zyn@seu.edu.cn).

Abstract: The pupil size is an important parameter in different studies on vision and ophthalmology. A pupil size estimation model is constantly needed when actual measurements are unavailable. The reported pupil estimation models commonly adopt the product of light intensity and viewing field area, supposing the light contributes uniformly across the spatial domain. In this paper, the pupil diameters were measured for stimuli with different intensities and different sizes. Spatially varying effect were observed, especially for large field stimuli and annular bright stimuli. A spatially weighted flux density is proposed which shows a high correlation with pupil diameters. A hyperbolic equation is fitted to estimate the natural pupil diameter with independent light spatial distributions. The goodness of fit R^2 reaches 0.97. The accuracy of the model is further verified with a natural indoor scene for different viewing distances and different illumination levels. The model predicted pupil diameters show a high correlation with the measured data.

Index Terms: Pupil Size, corneal flux density, display luminance, light environment, visual optics.

1. Introduction

As an important part of the eye, the pupil controls the amount of light that enters our eye by changing its size. It naturally enlarges and contracts based on the intensity of the light around [1], [2]. The pupil size has a large effect on the perception of brightness [3] and other visual functions, like the modulation transfer function of the eye, *et al.* [4], [5]. It is also an indispensable parameter for photobiological safety evaluation since the radiant flux that enters the eye is proportional to pupil area [6]. In some ophthalmological clinical testing, pupil size could have significant effects on the indicators like the flicker electroretinograms [7], [8]. In visual perceptual experiments, pupil size could be an important control parameter which needs to be considered to get a constant troland value [9], [10]. Besides, pupil size affects many performances in near-eye displays such as Maxwellian view optical systems, light field systems [11]. For these reasons, it is often desirable to estimate the pupil size for a given set of conditions when actual measurements are unavailable.

Based on available data, various formulas have been proposed to predict the pupil diameter. It is widely agreed that pupil size depends mainly on the adapting luminance and the field size, and modulated by other factors like the observers' age, monocular versus binocular stimulation, etc [12]. Under photopic light levels, Stanley and Davies demonstrated that the pupil was a simple

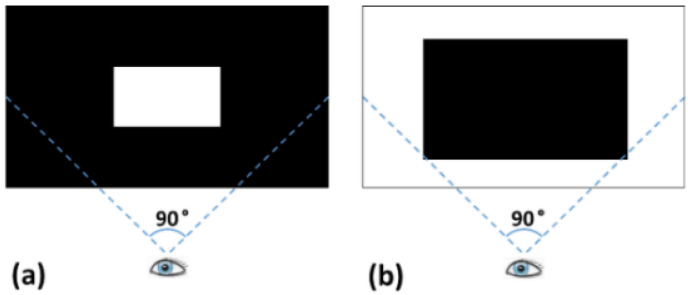

Fig. 1. Testing pattern displayed on the screen to simulate the light stimuli with different spatial distribution. (a) Centre-bright-rectangular-pattern. (b) Centre-dark-annular-pattern.

flux integrator for field size between 0.4° and 25.4° [13]. It was supported by Atchison *et al.* for both mesopic and photopic lighting levels that if corneal flux density (product of luminance and field size, in unit of cd/m^2•deg^2) kept constant there will be no change in pupil diameter for sizes of the stimulus field up to 24° [14].

However, there is little experimental analysis on the influence of detailed spatial luminance distribution, since the reported experimental data were based on stimuli of uniform illumination surfaces, which are different from actual scenes. Furthermore, even for the uniform illumination stimuli, it is unclear whether the current models using corneal flux density determining pupil size still applies when the stimuli are much larger. In currently fast-developing virtual reality and augmented reality headsets, most have field of view larger than 25.4° [15]. In fact, the earliest study by Ferree *et al.* indicated that the correlation between corneal flux density and pupil size deviated for stimuli with 40° or larger field sizes [1].

So in this paper, a perceptual experiment was first implemented to evaluate the spatial influence with large field of view and patterned stimuli, which would be illustrated in session 2. The experimental results would be presented in Session 3. Based on these data, a pupil size estimation model would be built up in session 4. A verification experiment would be addressed in session 5. And finally a conclusion would be made in session 6.

2. Experiment

2.1 Experiment Stimuli

Since the stimuli sizes experiments reported were generally within the range of 25°, in this paper different stimuli sizes were applied up to the range of 90° × 63°. Besides, annular illumination patterns with darken center regions were applied as the stimuli (see Fig. 1). Considering that most of the current instruments and devices representing light environment measurement output with two-dimensional matrix data, rectangular stimuli were adopted in our experiments, so as to facilitate the acquisition and processing of light environment data in practical applications.

2.2 Experimental Setup

A total of 99 stimuli were presented combining different illumination intensities and pattern sizes. For the centre-bright- rectangular-pattern, there were 54 stimuli of 9 luminance levels (20, 40, 60, 80, 100, 150, 200, 300 and 500 cd/m^2) combined with 6 stimuli sizes (10° × 7°, 20° × 14°, 30° × 21°, 40° × 28°, 60° × 42°, and 90° × 63°). For centre-dark-annular-patterns, there were 45 stimuli of 9 luminance levels (20, 40, 60, 80, 100, 150, 200, 300 and 500 cd/m^2) combined with 5 darken region sizes (10° × 7°, 20° × 14°, 30° × 21°, 40° × 28°, 60° × 42°). These stimuli were generated with an 80-inch LCD panel (SHARP LCD-80X818A). With grayscale calibration, the color temperature of the testing gray pattern was set to D65 and the luminance variation was suppressed lower than 3% within the viewing field [16], [17]. Each stimulus was presented for 15 seconds, which was

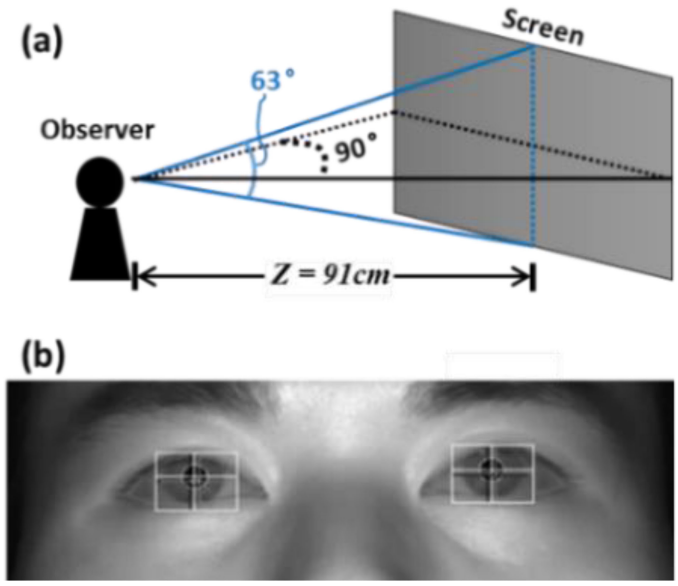

Fig. 2. (a) Experimental setup. (b) Pupil status recorded by the infrared eye tracker.

supposed to keep the pupil size steady [18], [19]. The 99 stimuli were divided in 4 groups to shorten the experiment duration, and before each group 5 minutes were taken for dark adaption.

The subjects were sitting 91 centimeter away from the screen, and were asked to look at the center of screen (see Fig. 2). Infrared eye tracker RED250 by German SMI Company was used to track the subject eye to check the subject was staring at the screen center. Meanwhile, the pupil state was captured by the eye tracker and the pupil diameter were calculated and provided by its built-in software tool BeGaze [20]. See Fig. 2.

2.3 Subjects

Eight subjects attended the experiment, including 4 male and 4 female Chinese aged between 20 and 30 years. All the subjects had 20/20 or better visual acuities and were in good ocular and systemic health. The experiment was approved by the Visual Perception Research Ethics Committee of the Joint International Research Laboratory of Information Display and Visualization, Southeast University. All the subjects gave written informed consent. Each subject repeated the experiment twice to observe the consistency of the data before and after. The average value for the both eyes were used for modeling, so there are 16 sets of data recorded for each stimulus.

3. Results

Fig. 3 shows the data gathered in the experiment for the centre-bright-rectangular-patterns. All the points are the average of 8 observers. Different lines represent different illumination sizes. The results show the familiar relationship between pupil diameter and stimuli luminance. The pupil diameter contracts as the luminance increases. Besides, there is a strong interaction between the stimuli size and its effect on the pupil diameter, larger sizes producing more pupil contraction. But the effect of stimuli size on pupil diameter is getting reduced as the stimuli size is bigger.

Fig. 4 shows the data gathered in the experiment for centre-dark-annular-patterns. It is verified again that the pupil diameter contracts as the luminance increases. Also, as the dark region size increase, the active bright area decrease, and then the pupil size dilates.

For the centre-dark-annular-pattern stimuli with $60^\circ \times 42^\circ$ dark area, the active area is 90×63-$60 \times 42 = 3150$ deg^2, while compared with centre-bright-rectangular-pattern with the area 60×42

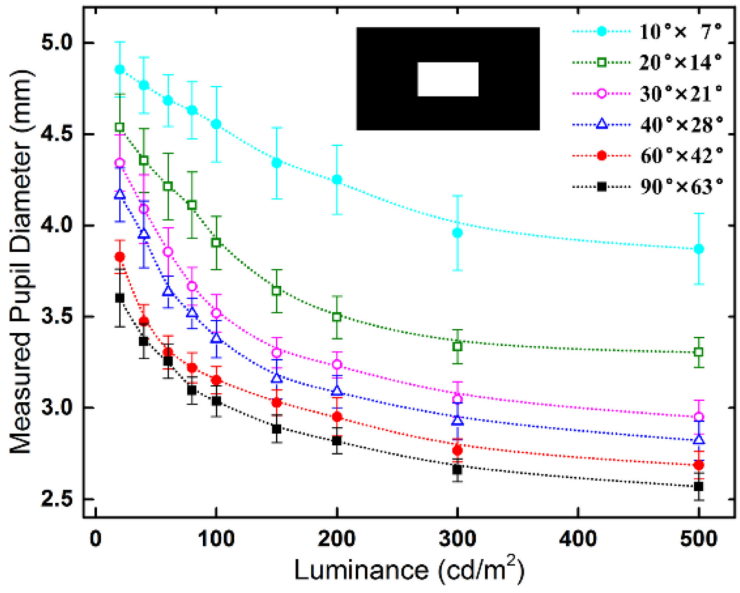

Fig. 3. Recorded pupil diameters changing with stimuli luminance with different bright region areas for centre-bright-rectangular-pattern. The error bars indicate 95% confidence intervals.

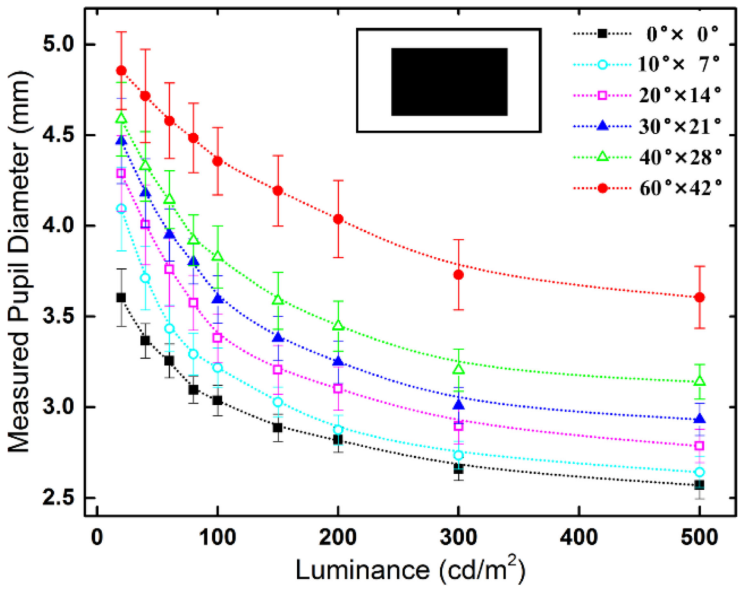

Fig. 4. Recorded pupil diameters changing with stimuli luminance with different dark region areas for centre-dark-annular-patterns. The error bars indicate 95% confidence intervals.

$= 2520$ deg^2 (both are indicated with red round dots in Fig. 4 and Fig. 3 separately), if the luminance is the same, the former stimulus has larger corneal flux intensity and should result in smaller pupil size. But the experimental data presents the opposite result. Fig. 5 shows the experimental recorded pupil diameters as a function of calculated corneal flux density. For center bright rectangles smaller than $40° \times 28°$, there was a strong correlation between pupil diameter and corneal flux density, as shown with the black square dots in Fig. 5. When looking at the red data for $60° \times 42°$ and the green data for $90° \times 63°$ center bright stimuli, it was found that as the stimuli area increases,

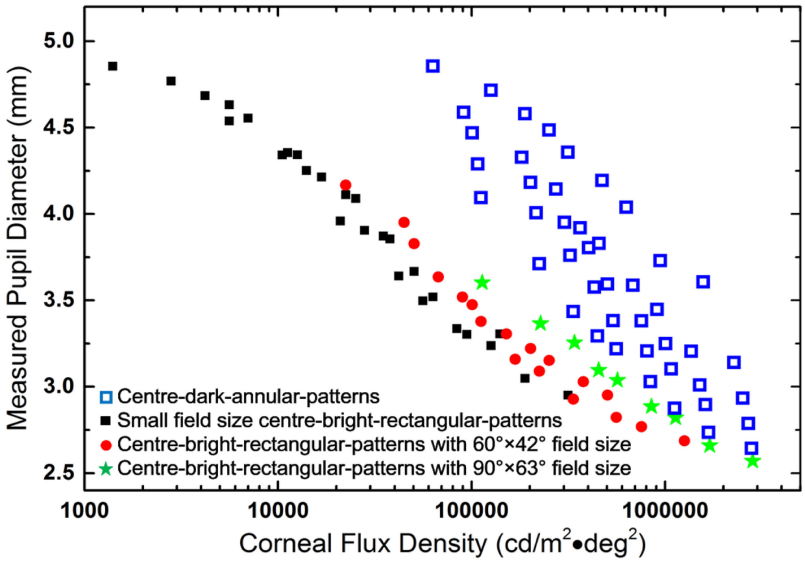

Fig. 5. The experimental recorded pupil size as a function of calculated corneal flux density.

the data became more deviated from the trend line. Such deviation is especially evident for the center-dark-annular-patterns, as shown with the blue hollow dots in Fig. 5. The deviation will be more obvious if linear scales are used.

4. Modeling

As mentioned, data for large field size centre-bright-rectangular-patterns and data for centre-dark-annular-patterns deviate from the trend line fit for the relatively small size stimuli. More specially, the corneal flux density seems to be over calculated for those large field size stimuli or center dark annular stimuli. We consider introducing a weighting function to weight the light stimulation and then the contribution to the corneal flux density according to the spatial locations,

$$\overline{F} = \iint L\left(\theta_x, \theta_y\right) \cdot w\left(\theta_x, \theta_y\right) d\theta_x d\theta_y \tag{1}$$

where $\overline{F}w(\theta_x, \theta_y)$ s the spatially weighted corneal flux density, $L(\theta_x, \theta_y)w(\theta_x, \theta_y)$ s the luminance distribution in latitude-longitude coordinates, an $w(\theta_x, \theta_y)$ is the spatial weighting function. As most commercial optical instruments represent the measured data in rectangular coordinates, it is preferred to use luminance distribution in rectangular coordinate. We try the most typical Gaussian function for weighting and rewrite eq. (1) accordingly:

$$\overline{F} = \iint L\left(x, y\right) \cdot e^{-\frac{x^2+y^2}{2\cdot\sigma^2}} \cdot \frac{1}{\left(1+x^2\right)\left(1+y^2\right)} dxdy \tag{2}$$

where $L(x, y)$ is the luminance distribution in rectangular coordinates. For convenience, x, y are normalized by the vertical viewing distance, by setting $Z = 1$ (see Fig. 2), then $\theta_x = \arctan(x)$, $\theta_y = \arctan(y)$, after derivation there is a factor $\frac{1}{(1+x^2)(1+y^2)}$ in eq. (2). The same form of hyperbolic equation as Stanley and Davies used is applied to fit the relationship between the pupil diameter D and the spatially weighted corneal flux density $\overline{F}$ [13]. By nonlinear optimization of experimental data in Fig. 5, the quantified formula is obtained:

$$D = \mathbf{5.12} - \mathbf{2.76} \cdot \left(\frac{\left(\bar{F}/\mathbf{2506}\right)^{\mathbf{0.8}}}{\left(\bar{F}/\mathbf{2506}\right)^{\mathbf{0.8}} + \mathbf{10}} \right) \tag{3}$$

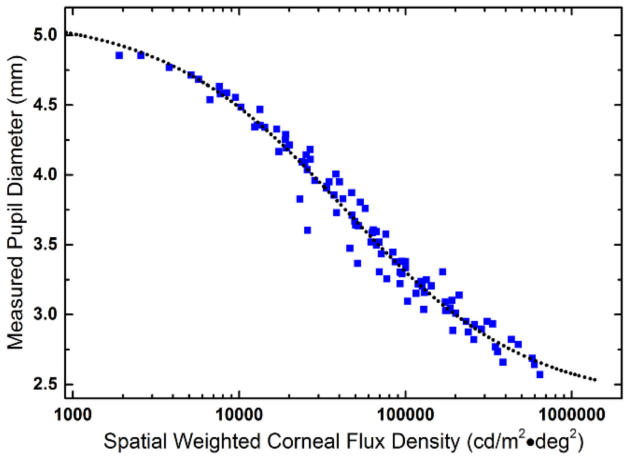

Fig. 6. The experimental recorded pupil size as a function of spatially weighted corneal flux density. The scattered dots are for all the measured data in Fig. 5. The dashed curve is for eq. (3).

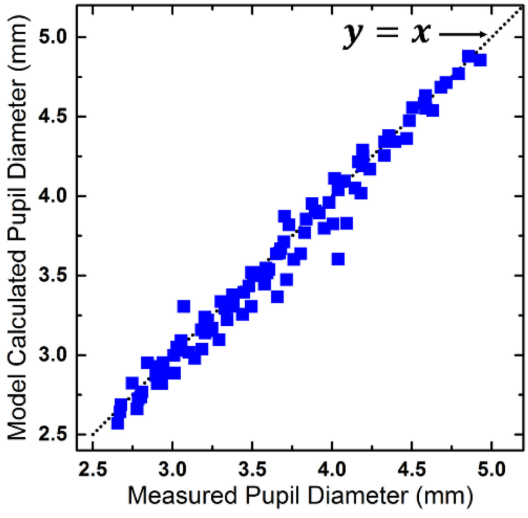

Fig. 7. The correlation between the model calculated data and the measured data for the modeling experiments. The scattered dots are for all the measured data in Fig. 5.

In this case, σ in eq. (2) is 0.27. The relationship between the measured pupil diameters and the calculated spatially weighted corneal flux densities with eq. (2) is represented in Fig. 6. The correlation became much more concentrated and convergent. The dashed line in Fig. 6 is the fitting curve of eq. (3). The goodness of fitting based on eq. (3) was $R^2 = 0.97$.

Therefore, based on equations (2) and (3), the pupil size of the observer can be easily and accurately estimated by measuring the optical distribution $L(x, y)$ within the visual field. Fig. 7 further reflects the correlation between the model estimated and actual measured data.

5. Verification

To further evaluate the accuracy of the model, a nature indoor scene with different viewing distances and different ambient illumination levels is used. See Fig. 8. Lighting environment includes 0 *lux* (Dark), 150 *lux* (Middle) and 300 *lux* (Bright), with the color temperature of 5500 K. The observation distance includes twice, three times and four times the screen height, namely 1.44 m (2 H), 2.16 m (3 H) and 2.88 m (4 H). The panel presents full screen grayscale image with six luminance levels

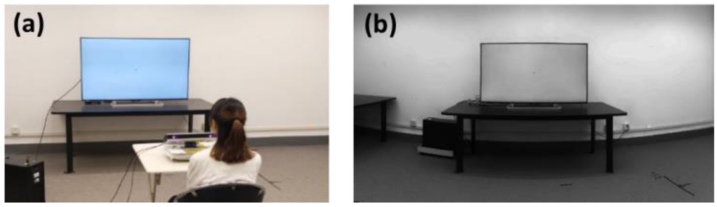

Fig. 8. A nature indoor scene tested for model evaluation. (a) The scene for the verification experiment. (b) A measured light distribution.

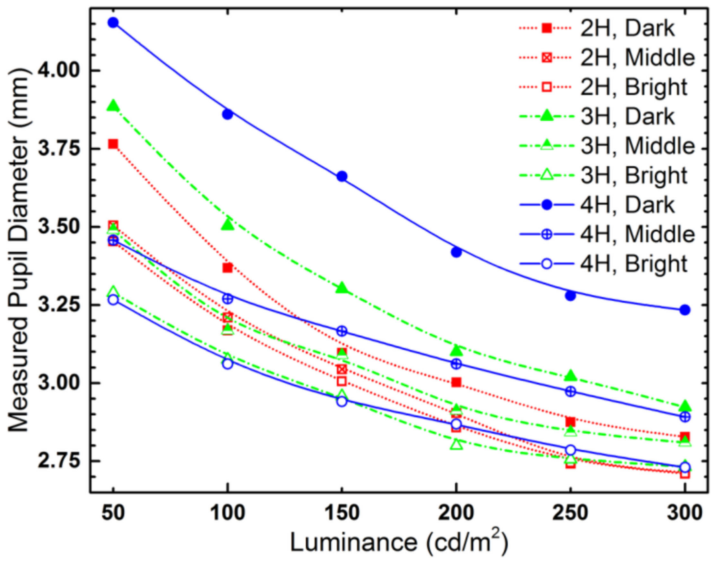

Fig. 9. Measured pupil size as a function of luminance for an indoor scenario with different viewing distance and different illumination levels.

including 50, 100, 150, 200, 250, and 300 (cd/m^2). Fig 8(b) shows a measured luminance distribution recorded by HDMS-200 developed by Southeast University which supports the light distribution measurement within the field range up to 120° × 90°.

Another six subjects attended the verification experiment, including 3 male and 3 female aged between 20 and 30 years. Fig. 9 shows the average measured pupil diameters for different settings. It is observed that with longer viewing distance, the screen contributes less in viewing angle area, and then the ambient light has more significant effect on pupil size. It is why the blue lines with circle points are flatter and sparser.

The luminance distribution $L(x, y)$ within the 120° × 90° field size was measured for each setting, and then the pupil diameters were calculated by the model with eq. (2) and (3). The model calculated results were compared with the actual measured pupil diameter in Fig. 10. There is a high correlation between the model calculation values and the measured data. The fitting goodness to the line $y = x$ was $R^2 = \mathbf{0.94}$. This shows that in the actual scenario the model proposed for pupil diameter estimation is reliable, even with different viewing distance or different ambient illumination levels. The model provides a useful approach to estimate the pupil size when direct measure of pupil is not available, like in the light environment design stage or for photobiological safety assessment. It also provides a practical model for bionic eye design.

It is well known that ambient light environments have significant effects on visual performances and comfortness. Normally ambient light conditions are characterized with illuminance in lux, like the verification experiment in this paper, but the visual display terminals are characterized in luminance

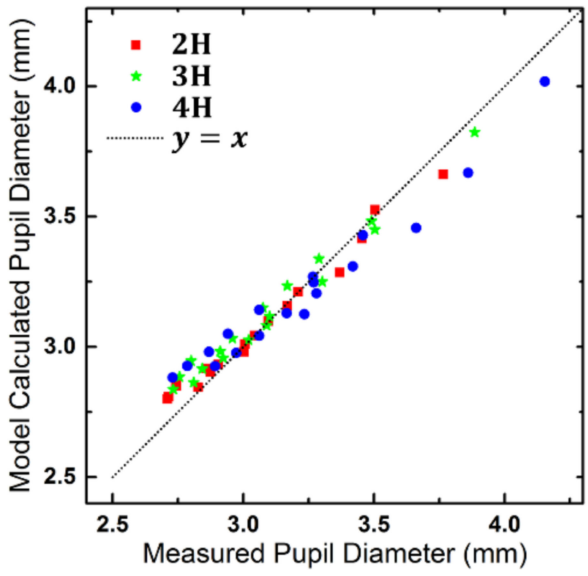

Fig. 10. Model calculated pupil diameter versus measured pupil diameter for indoor scenario.

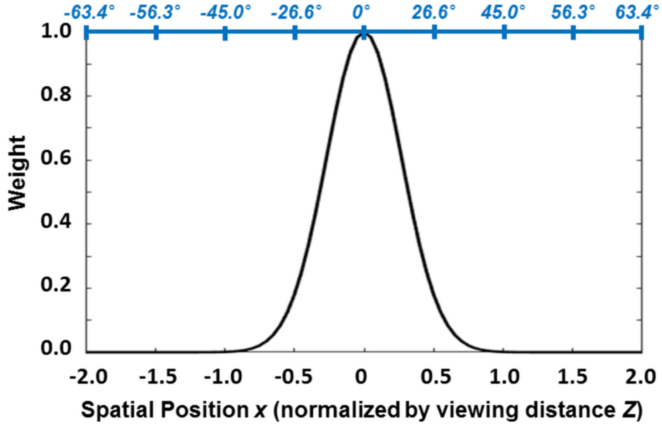

Fig. 11. The Gaussian weighting function proposed in the model. The weight varies in x direction ($y = 0$). The top axis indicates the corresponding viewing angles.

in cd/m^2. This combination makes perceptual experiment statistical analysis and modeling much complicated. The result above shows a possibility that by using only the luminance values entering the eye, the visual response of pupil size could be comprehensively characterized. Actually in this paper, the ambient light information is included in the luminance values in the effective viewing field, like taking account of the luminance values of the wall which reflects the ambient light.

It is important to note that the data analyzed in this paper were mainly for photopic light levels as the most common visual scene. Caution should be taken when trying to extend the model to scotopic conditions. Also D65 white illumination is used for modeling and 5500 K light environment is used for scenario check, but the effect of color still needs to be thoroughly studied for the future work. With regression, the Gaussian weighting function provides a good result, and the full width at half maximum is 0.27 (close to *tan*(15°)). Fig. 11 shows the Gaussian weighting function used in Eq. (2). The trend is consistent with Stiles and Crawford's early work, known as Stiles-Crawford effect [21]. However, this does not acknowledge many of the subtleties of pupil control, such as the contribution of rod and cone systems, their respective spectral sensitivities and interaction

between them. Data for this paper were based on the subjects aged between 20 and 30 years. When necessary, the age effect function proposed by Watson and Yellott provides a quantitative approach to adjust the estimated pupil diameter to other age ranges [12].

6. Conclusions

As a conclusion, a spatially weighted flux density was proposed which shows a high correlation with observer pupil diameter. A single hyperbolic equation was fitted to estimate the natural pupil diameter with independent light spatial distribution. The R^2 of fitting is 0.97 for model building and 0.94 for real scenario validation. The pupil diameter estimation model applied 2D luminance spatial distribution $L(x, y)$ in rectangular coordinates as the input parameter compatible with commercial optical instruments or softwares. This model would be helpful when pupil size needs to be known while direct measurement is not available, like in the light environment design stage or for photobiological safety assessment. It also provides a reference for bionic eye design.

Acknowledgment

The authors would like to thank all the subjects for their time attending the experiment.

References

[1] C. E. Ferree, G. Rand, and E. T. Harris, "Intensity of light and area of illuminated field as interacting factors in size of pupil," *J. Exp. Psychol.*, vol. 16, pp. 408–422, 1933.
[2] B. H. Crawford, "The dependence of pupil size upon external light stimulus under static and variable conditions," *Proc. Roy. Soc. B*, vol. 121, pp. 376–395, 1936.
[3] D. Valente and B. Vohnsen, "Retina-simulating phantom produced by photolithography," *Opt. Lett.*, vol. 42, pp. 4623–4626, 2017.
[4] S. Ravikumar and L. N. Thibos, "Calculation of retinal image quality for polychromatic light," *J. Opt. Soc. Amer. A*, vol. 25, pp. 2395–2407, 2008.
[5] J. Rovamo and H. Kukkonen, "Foveal optical modulation transfer function of the human eye at various pupil sizes," *J. Opt. Soc. Amer. A*, vol. 15, pp. 2504–2516, 1998.
[6] K. Schulmeister and J. Daem, "Risk of retinal injury from "Risk Group 2" laser illuminated projectors," *J. Laser Appl.*, vol. 28, 2016, Art. no. 042002.
[7] K. Kato, M. Kondo, M. Sugimoto, K. Ikesugi, and H. Matsubara, "Effect of pupil size on flicker ERGs recorded with RETeval system: New mydriasis-free full-field ERG system," *Invest Ophthalmol Vis. Sci.*, vol. 56, pp. 3684–3690, 2015.
[8] L. Fang, Y. Wang, and X. He, "Effect of pupil size on residual wavefront aberration with transition zone after customized laser refractive surgery," *Opt. Exp.*, vol. 21, pp. A1404–A1416, 2013.
[9] C. Q. Davis, O. Kraszewska, and C. Manning, "Constant luminance (cd/m2) versus constant retinal illuminance (td·s) stimulation in flicker ERGs," *Documenta Ophthalmol*, vol. 134, pp. 75–87, 2017.
[10] L. N. Thibos, N. Lopez-Gil, and A. Bradley, "What is a troland," *J. Opt. Soc. Amer. A*, vol. 35, pp. 813–816, 2018.
[11] R. J. Jacobs, I. L. Bailey, and M. A. Bullimore, "Artificial pupils and Maxwellian view," *App. Opt.*, vol. 31, no. 19, pp. 3668–3677, 1992.
[12] A. B. Watson and J. I. Yellott, "A unified formula for light-adapted pupil size," *J. Vision*, vol. 12, no. 10, pp. 1–12, 2012.
[13] P. A. Stanley and A K. Davies, "Ophthal. The effect of field of view size on steady-state pupil diameter," *Physiol. Opt.*, vol. 15, pp. 601–603, 1995.
[14] D. A. Atchison, C. C. Girgenti, G. M. Campbell, J. P. Dodds, T. M Byrnes, and A. J. Zele, "Influence of field size on pupil diameter under photopic and mesopic light levels," *Clin. Exp. Optometry*, vol. 94, pp. 545–548, 2011.
[15] Z. He, X. Sui, G. Jin, and L. Cao, "Progress in virtual reality and augmented reality based on holographic display," *App. Opt.*, vol. 58, no. 5, pp. A74–A81, 2019.
[16] K. A. Fetterly, H. R. Blume, M. J. Flynn, and E. Samei, "Introduction to grayscale calibration and related aspects of medical imaging grade liquid crystal displays," *J. Digit. Imag.*, vol. 21, pp. 193–207, 2008.
[17] J. Wang, Y. Zhang, X. Li, and Y. Weng, "Color breakup visibility thresholds for 2-field sequential colors," *Color Res. Appl.*, vol. 42, pp. 580–590, 2017.
[18] J. Klingner, R. Lumar, and P. Hanrahan, "Measuring the task-evoked pupillary response with a remote eye tracker," in *Proc. Symp. Eye Tracking Res. Appl.*, 2008, pp. 69–72.
[19] I. J. Murray, J. Kremers, D. Mckeefry, and N. R. A. Parry, "Paradoxical pupil responses to isolated M-cone increments," *J. Opt. Soc. Amer. A*, vol. 35, pp. B66–B71, 2018.
[20] J. S. Tsukahara, T. L. Harrison, and R. W. Engle, "The relationship between baseline pupil size and intelligence," *Cogn. Psychol.*, vol. 91, pp. 109–123, 2016.
[21] W. S. Stiles and B. H. Crawford, "The luminous efficiency of rays entering the pupil at different points," *Proc. Roy. Soc. London Ser. B*, vol. 112, pp. 428–450, 1982.